SYNTHESIS OF CoFeCrMnNi/TiC-HIGH ENTROPY ALLOY COMPOSITE COATINGS BY ELECTRODEPOSITION TECHNIQUE

Shanmugavel Sudarsan, Mariappan Anandkumar,
Marina Samodurova, Sergey Lezhnev, Evgeniy Panin

South Ural State University, Chelyabinsk 454080
Russian Federation, sergey_legnev@mail.ru (S.L.);
shanmugavels@susu.ru (S.S.); anandkumarmariappan@susu.ru (M.A.);
samodurovamn@susu.ru (M.S.); sergey_legnev@mail.ru (S.L.); cooper802@mail.ru (E.P.)

Received 02 November 2024
Accepted 13 January 2025 *DOI: 10.59957/jctm.v60.i3.2025.6*

ABSTRACT

CoFeCrMnNi high entropy alloys (HEA) composite coating containing various weight fractions of titanium carbide (TiC) was electrodeposited over a copper substrate using an electrodeposition technique. The current work to investigate the synthesis of HEA-TiC composite coatings through simple and convenient process. The X-ray diffraction (XRD) measurement confirms the presence of single-phase HEA/TiC composite coating comprising of FCC and BCC phase. In addition, the fabricated coating material has a rough surface with five elements and TiC uniform dispersion confirmed by scanning electron microscopy- Energy-dispersive X-ray spectroscopy (SEM-EDS). Specifically, these results revealed the better properties of HEA-TiC composite coatings were achieved within short duration and simple technique.

Keywords: high entropy alloy composite coatings, electrodeposition, titanium carbide, microcracks.

INTRODUCTION

High entropy alloys (HEA) are a novel type of metallic substances which has got a lot of interest from scientists in the past few decades due to it is unique structure. They are producing a unique fabrication method. Unlike usual alloys, these multicomponent constituents include no dominant elements, which are made up of five or more principal elements in near equimolar composition. Due to their high mixing entropy, HEA frequently forms simpler solid solution systems. High entropy effects had an impact on HEA structure and properties. Hence, the field of HEA has substantial attention in different material science section and engineering applications [1 - 5]. Recently, HEA have received significant research, and several alloy compounds were reported with good strength, corrosion resistance and wear resistance characteristics etc. The structure of these alloy compositions makes them appropriate for usage in functional materials. A notable property of HEA is their incredible capacity to retain their crystal structure despite exposure to extreme temperatures [6, 7].

TiC particles are among the toughest metal carbides with the benefits of high melting temperature (3420 K) and low density (4.95 g cm^{-3}). TiC possesses superior properties such as great bending strength, fracture toughness, very good wear and corrosion resistance. It exhibits excellent thermal stability and electrical conductivity. It deliberated as a favourable material for coating reinforcement that can enhance the inclusive achievement for coatings of composites [8]. Furthermore, the incorporation of TiC particles on the metal matrices could substantially improve alloy characteristics. Similarly, synthesis and microstructure of different TiC composites has also been discussed [9, 10]. Aforementioned, metal-reinforcement particles based composite coatings reveal broad range of characteristics to converge distinct requirements such as increased mechanical behaviour, greater wear and

corrosion protection; these properties create exemplary novel uses in various fields such as defence, automobile, aerospace and nuclear power industries etc [8]. Hence, HEA-TiC composite coatings are expected to have broad applications.

Earlier, the preparation of HEA-TiC composite coatings was predominantly fabricated using induction furnace smelting [11], melting-casting [12], mechanical alloying and rapid solidification [13], magnetron sputtering [14], laser cladding [15], thermal spray [16] etc. The fundamental issue with these coating processes, on the other hand, is their ability to be applied under temperature settings. Most of the laser coating is very reactive to cracks, causing the coating to fracture. The thermophysical characteristics of the metal matrix and ceramic phase differ significantly [17]. Electroless-plating process has possessed greater potential, but it is more costly compared to electrodeposition process. The use of electroless-plating is inadequate to fulfil the feasibility applications in peculiar area [18].

However, the electrodeposition process is an effective, simple, convenient, fast coating and one-step process without the need of extra heat treatment [19]. In addition, HEA composite coating can be fabricated at a lower temperature which is cost effective and smooth surface. This is primarily owing to the intricate nature of the electrochemical bath, which contains several metallic precursors. Composite coating with an excellent bonding existing between the reinforcement particles and metals. As of now, no study has been made on electrodeposition of TiC particles on HEA to form a composite coating.

In compliance with Yoosefan et al., developed CoCrFeMnNi-HEA coatings via electrodeposition in dimethyl formamide/methyl cyanide (DMF/CH_3CN) condition and it exhibits potential application in corrosion resistance behaviour [20]. Corrosion resistance behaviour has discussed by Popescu et al., for CoCrFeMnNi-HEA thin films system [21]. Oliveira et al. also described the NieWeCo alloys achieved by electrodeposition in a specific pH and current density [22]. More research is needed on preparing HEA composite coating with different reinforcement particles using electrodeposition coating method. In the current study, electrodeposition of HEA-TiC composite coatings was synthesized employing various concentrations of TiC particles.

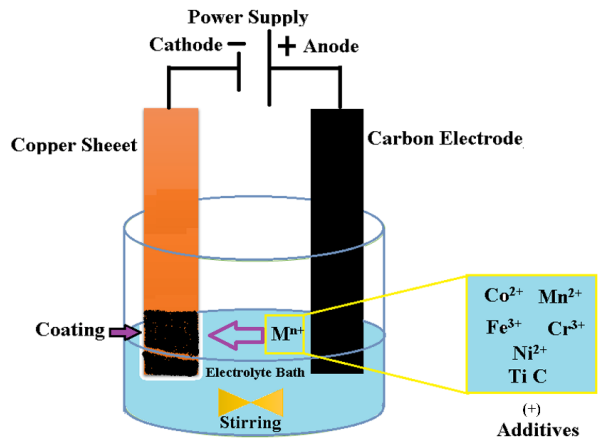

Fig.1. Schematic diagram of electrodeposition setup for the fabrication of HEA and HEA-TiC coating on Cu sheet.

EXPERIMENTAL

The electrodeposition HEA-TiC composite coatings were done using KA3005D digital control DC power source (30 V, 5 A) device. Aliyu-Srivastava approach has been followed with some modification [23]. Copper sheet was carefully gleaming off to 2500 grit utilized SiC abrasive sheets. Copper was selected as a cathode (3 × 2 × 0.5 cm) and was washed in 10 weight percentage HCl at lukewarm condition for 5 s, again cleaned with demineralized water. Various constituents were used as additives in electrochemical bath to enhance the surface morphology while pH 1.5 was maintained using a solution of NaOH. Electrodeposition was carried for 15 min with a graphite rod as anode (5 x 1 × 1 cm). After deposition, the coating substrate was washed with purified water and dried at lukewarm condition. The investigation was conducted through varying the content of TiC particles (0.5 g, 1 g, 3 g, 5 g and 7 g / 100 mL) in electrochemical bath, and the coatings are named as HEA-TiC0.5, HEA-TiC1, HEA-TiC3, HEA-TiC5 and HEA-TiC7 respectively.

Electrodeposition of CoFeCrMnNi-HEA coatings on cleaned copper sheets were achieved in different parameters as given in Table 1. In the electrolyte bath, the additives such as sodium dodecyl sulphate (0.25 g / 100 mL) ($C_{12}H_{25}O_4SNa$) assisted to develop metallic ions into the coatings, ascorbic acid (0.5 g / 100 mL) ($C_6H_8O_6$) was used to increase the coating

Table.1. Electrodeposition bath composition with different parameters of HEA and HEA-TiC composite coatings.

Compound code	Bath composition	Concentration, g L^{-1}	Conditions
HEA	$MnCl_2.4H_2O$	357.5	pH = 1.5
	$NiCl_2.6H_2O$	17.5	Temperature = 30°C
	$CoCl_2.6H_2O$	5	Deposition time = 15 min
	$FeCl_3.6H_2O$	7.5	Voltage = 5 V
	$CrCl_3.6H_2O$	350	Stirring speed = 200 rpm
	HEA-TiC.5	0.5 g /100 mL	
	HEA-TiC1	1 g /100 mL	
	HEA-TiC3	3 g /100 mL	
	HEA-TiC5	5 g /100 mL	
	HEA-TiC7	7 g /100 mL	

closeness, boric acid (4.5 g / 100 mL) (H_3BO_3) behave as buffering agent, potassium chloride (12 g / 100 mL) (KCl) was utilized to enhance the coating morphology, sulfanilic acid (0.5 g / 100 mL) ($C_6H_7NO_3S$) was used in the formation of the uniform coating and formic acid (0.5 mL / 100 mL) (CH_2O_2) was utilized to enhance the nature of surface of HEA-TiC coatings. Continuous magnetic stirring was carried out in order to maintain a uniform TiC particles concentration during the electrodeposition process. The schematic representation of electrodeposition of HEA-TiC composite coatings setup was represented in Fig.1.

The phase evolution of the coated HEA and HEA-TiC composites was explored by XRD (Rigaku Ultima IV, Rigaku) utilizing Cu-Kα radiation (λ = 0.15406 Å) from 2 theta 20 to 95° at a scan speed of 2° per min. FESEM photos were captured utilizing JEOL JSM7001F scanning electron microscope (SEM). The elemental mapping and atomic percentage of elements were analysed using Energy-dispersive X-ray spectroscopy (EDS) (Oxford Instruments, UK).

RESULTS AND DISCUSSION

The XRD results of CoFeCrMnNi HEA and HEA-TiC composite coatings is shown in Fig.2a. A combination of FCC and BCC phases were observed in all the samples. The diffraction peaks at 43.29°, 50.41° and 74.07° corresponds to the (111), (020) and (022) of the FCC phase (Fm-3m, ICDD card number: 96-901-1624). All the HEA-TiC composite coatings showed BCC phase which is due the formation of some impurities. Zhao et al., 2022 also observed similar kind of results in FeCoNiCrMn high entropy alloy film which was used as an excellent protective coating application [23]. Similar kind of results were discussed in the coating of graphene oxide on MnCrFeCoNi coating system [24]. The obtained result proposes that the as-deposited alloys were crystalline nature.

The typical peaks of TiC particles of enlarged diffracted peaks is shown in Fig. 2b, representing the assimilation of different portion of TiC particles on a HEA matrix. The diffracted peaks observed at 2 theta 16.95°, 36.24°, 44.70°, 35.12°, and 60.45° corresponds to (222), (020), (111), (131), and (022) planes of the FCC phase (Fm-3m, ICDD card number: 96-901-2565) by the addition of TiC particles. Same kind of peaks has been noticed in Ni-TiC composite coatings. From the above composite coating, the position of maximum peaks of TiC was not altered, indicating that the crystal structure is oriented in the composite coatings. Furthermore, when the amount of TiC particles was increased from 0.5 g to 7 g, the diffraction peaks also increased which relates to the existence of TiC particles appeared in HEA-TiC composite coating samples [25, 26].

Low magnification SEM micrographs of HEA-TiC samples at various amount of TiC is shown in Fig. 3 (a, c, e, g, i and k) while high magnification of SEM images is shown in Fig. 3b, d, f, h, j and l. The acquired SEM pictures reveal that all the HEA-TiC composite coatings contain distinct coarse and

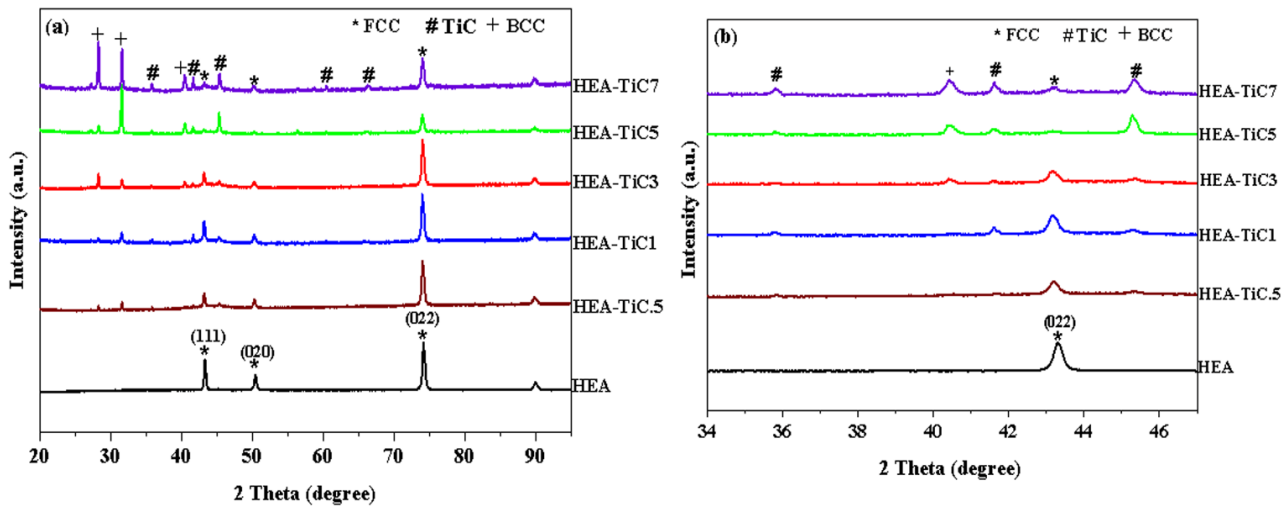

Fig. 2. XRD pattern of HEA and HEA-TC composite coating with an increasing amount of TiC (a), enlarged XRD pattern (b).

microcracks morphology along with the increase in the concentration of TiC particles. The development of internal stress during coatings of HEA causes the formation of microcracks and it is due to the evolution of hydrogen gas during electrodeposition composite coating process [27]. The development of microcracks by interstitial mechanical contact between the layer of coating and copper base, which reduces the size of the crystallite size [28]. Hence, the evolution of hydrogen gas can play a vital role in causing microcracks creation within the sample layers.

As the above micrographs indicates, that the presence of TiC particles on HEA-TiC coating samples has greater effect on the surface morphology of the resultant coating. When the addition of TiC 0.5 g / 100 mL causes more cracks and roughness on the surface morphology. Further, when the addition of TiC particles increased, the surface morphology of the film gets affected resulting in larger microcracks and high roughness. The uneven deposition coating and agglomeration were seen as the concentration of TiC particles increased from 0.5 g / 100 mL to 7 g / 100 mL. Despite this, SEM photographs at high magnification in Fig. 3 (b, d, f, h, j, and i) make it difficult to clearly detect the combination of the substrate and TiC particles due to their tiny size, polydispersity, and spherical shape. Benea et al has also discussed the influence of addition of TiC particles on their surface morphology in Ni matrix of hybrid through electro-co-deposition technique [29]. The distribution of concentration of TiC particles was unidentical within the HEA. It can be considered as the basic type of FCC and BCC phase due to the FCC nature of TiC particles. Similar type of results revealed in TiC reinforced FeCoNiCuA-HEA system with microstructure and tribiological properties [30].

As a result, the addition of varying concentrations of TiC particles to the copper surface matrix results in greater structural flaws and microcracks when compared to pristine HEA, as indicated by the perceived deviations in the SEM images. It is evident that the concentration of TiC particles affects the sample matrix and surface morphology.

EDS analysis on the deposited HEA coating revealed an even distribution of Co, Fe, Cr, Mn and Ni atoms as shown in Fig. 4. However, the appearance of Co and Cr atoms are more, while the existence of Fe, Ni and Mn remain less than the theoretical amount. It is primarily caused by the creation of a thin layer on the copper substrate in response to multiple variables such as pH, electrolyte bath concentration, temperature, and duration.

Similarly, in case of HEA-TiC composite coating, TiC is found to be evenly distributed over the HEA film (Fig. 5). Zhao et al. also revealed the results of elemental mapping of $Fe_{1.2}MnNi_{0.8}Cr$-HEA with TiC system [31].

The elemental composition (at. %) of HEA and HEA-TiC composite coatings (excluding TiC) is given in Fig. 6. In general, for HEA, the primary elements

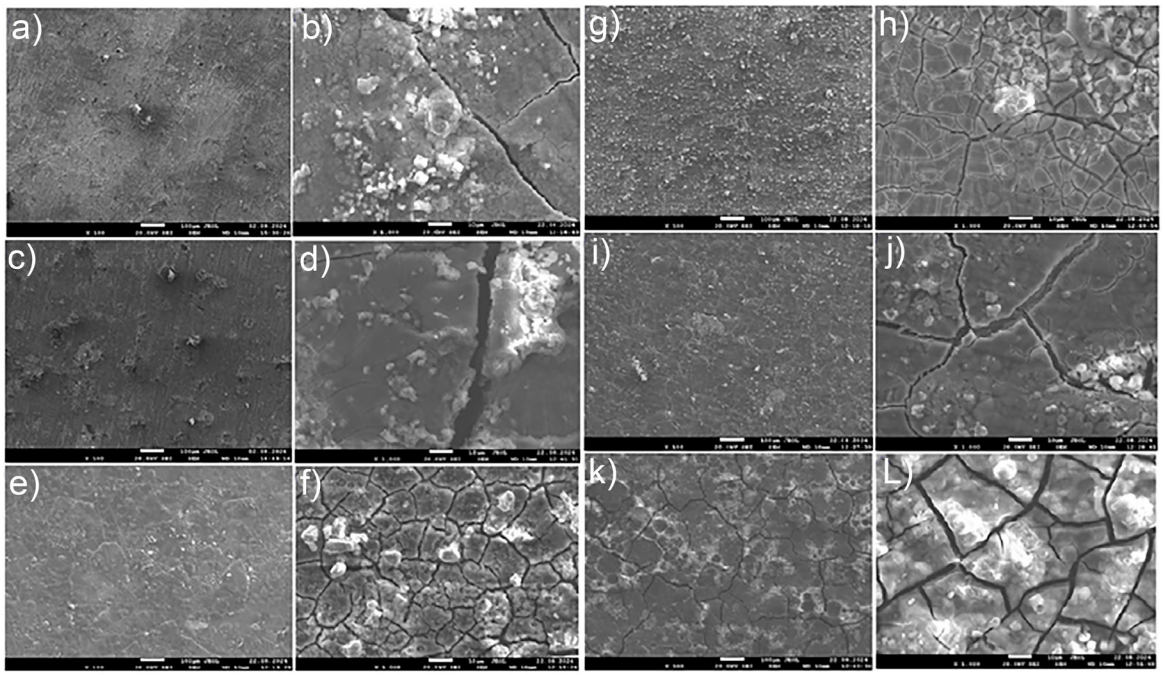

Fig. 3. SEM images of low and high magnification of HEA (a-b), HEA-TiC0.5 (c-d), HEA-TiC1 (e-f), HEA-TiC3 (g-h), HEA-TiC5 (i-j) and HEA-TiC7 (k-l).

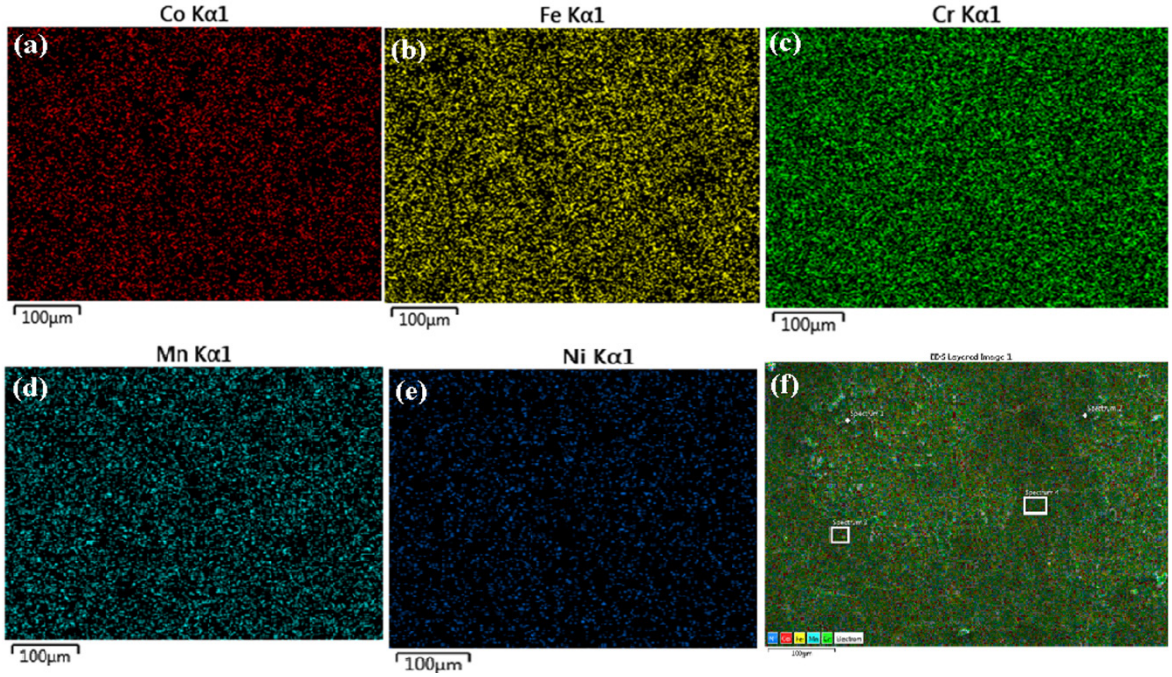

Fig. 4. EDS surface mapping of the HEA coatings.

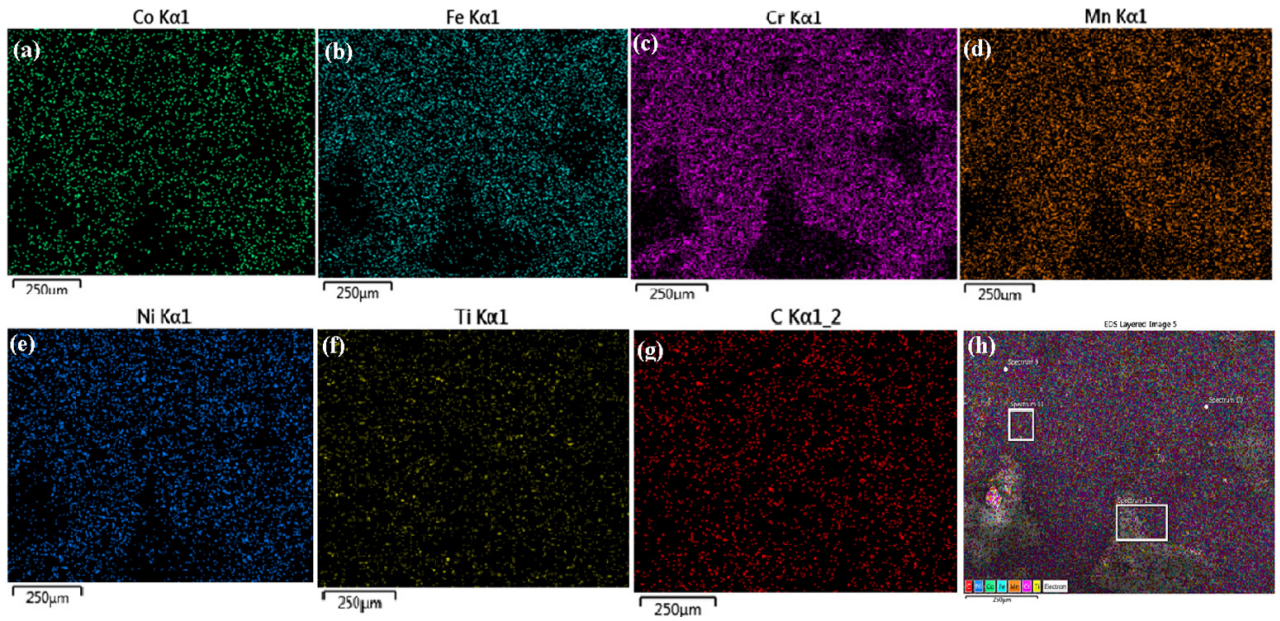

Fig. 5. EDS surface mapping of the HEA-TiC7 composite coatings.

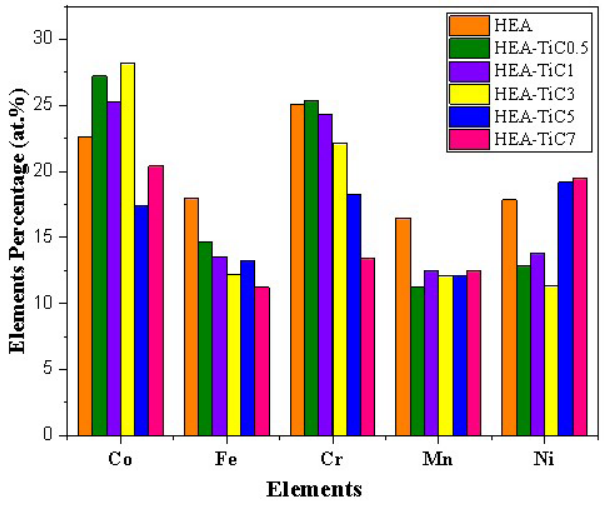

Fig. 6. Atomic percentage composition of HEA and HEA-TiC coatings utilizing SEM-EDS.

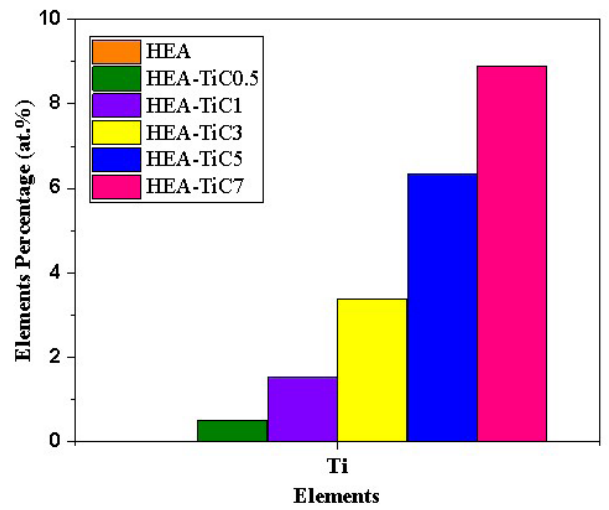

Fig. 7. Atomic percentage composition of HEA-TiC coatings utilizing SEM-EDS.

are predicted to be between 5 to 35 % [5, 28, 32]. As a result, Fig. 6 shows that all the coatings contain all five component elements in about equal atomic percentages. Similar reports deliberate on the findings of the CoCrFeNiMo high entropy alloy coating [33]. Fig. 7 shows the values of titanium content in the coatings calculated using EDS compositional assessment. In comparison with HEA without TiC, the titanium percentage of the coatings enhances from HEA to HEA-TiC7. The TiC content of the coatings resulting from the electrolyte bath improved as the TiC concentration increased.

CONCLUSIONS

In the present study, we have synthesized HEA composite coatings comprising of TiC particles by electrodeposition process. Microcracks and roughness surface morphology was observed with an increase in the concentration of TiC particles via SEM analysis. The XRD peaks were clearly supported the dispersion of TiC particles and the formation of FCC and BCC phases. An even dispersion of TiC particles within HEA and HEA-TiC composite coatings were perceived

using the elemental mapping and EDS analysis. The prepared HEA and HEA-TiC composite coatings via electrodeposition procedure is simple, less time and convenient coating technique.

Acknowledgements

The study was funded by a grant from the Russian Science Foundation № 20-19-00304, https://rscf.ru/en/project/20-19-00304/

***Authors contribution**: S.S. - conceptualization, methodology, writing - original draft; M. A. - resources, data curation; M. S. - funding acquisition, investigation, methodology, writing - review & editing, project administration; S. L. - investigation, software, validation; E. P. - visualization, formal analysis.*

REFERENCES

1. A.M.J. Popescu, F.Branzoi, I. Constantin, M. Anastasescu, M. Burada, D. Mitrică, V. Constantin, Electrodeposition, characterization, and corrosion behavior of CoCrFeMnNi high-entropy alloy thin films, Coatings, 11, 2021, 1367.
2. M.C. Gao, B. Zhang, S.M. Guo, J.W. Qiao, J.A. Hawk, High-entropy alloys in hexagonal close-packed structure, Metall. Mater. Trans. A., 47, 2016, 3322-3332.
3. G.B. Miracle, O.N.A. Senkov, critical review of high entropy alloys and related concepts, Acta Mater., 122, 2017, 448-511.
4. M. Vaidya, G.M. Muralikrishna, B.S. Murty, High-entropy alloys by mechanical alloying: A review, J. Mater. Res., 34, 2019, 664-686.
5. A. Aliyu, C. Srivastava, Microstructure and corrosion properties of MnCrFeCoNi high entropy alloy-graphene oxide composite coatings, Materialia, 5, 2019, 100249.
6. M. Mukarram, M. Mujahid, K. Yaqoob, Design and development of CoCrFeNiTa eutectic high entropy alloys. J.Mat. Res.Tech., 10, 2021, 1243-1249.
7. R. He, L. Yang, Y. Zhang, X. Wang, S. Lee, T. Zhang, A. Cabot, A CrMnFeCoNi high entropy alloy boosting oxygen evolution/reduction reactions and zinc-air battery performance, Ener. Stor. Mat., 58, 2023, 287-298.
8. H. Wang, X. Mao, Effect of attapulgite added in plating bath on the properties of Ni/TiC nano-composite coatings, J. Wuhan Univ. Tech. Mater. Sci. Ed., 32, 2017, 250-255.
9. M. Ma, W.C. Sun, Y.G. Zhang, X.J. Liu, Y.R. Dong, J.Y. Zi, Y. Xiao, Effect of TiC particles concentration on microstructure and properties of Ni-TiC composite coatings, Mat. Res., 22, 2019, e20190530.
10. M. Karbasi, N. Yazdian, A. Vahidian, Development of electro-co-deposited Ni-TiC nano-particle reinforced nanocomposite coatings, Surf. Coat. Tech., 207, 2012, 587-593.
11. W. Yu, Y. Wang, R. Li, R. J. Mao, Phase evolution, microstructure and mechanical property of AlCoCrFeNiTi high-entropy alloy coatings prepared by mechanical alloying and laser cladding, Met., 9, 2019, 1036.
12. Y. Guo, C. Li, M. Zeng, J. Wang, P. Deng, Y. Wang, In-situ TiC reinforced $CoCrCuFeNiSi_{0.2}$ high-entropy alloy coatings designed for enhanced wear performance by laser cladding, Mat. Chem. Phy., 242, 2020, 122522.
13. L. Zhicheng, K. Dejun, Effects of TiC mass fraction on microstructure, corrosive-wear and electrochemical properties of laser cladded CoCrFeNiMo high-entropy alloy coatings, Tribol. Int., 186, 2023, 108640.
14. D.D. Zhuang, W.W. Tao, B. Du, S.H. Zhang, X.L. Lian, F. Wang, Microstructure and properties of TiC-enhanced CrMnFeCoNi high-entropy alloy coatings prepared by laser cladding, Tribol. Int.,180, 2023, 108246.
15. M. Xiao, S. Nai, S. Nan, C. Feng, Z. Guan, C. Huo, G. Li, Preparation, mechanical properties and wear resistance of dual-sized TiC particles reinforced high-entropy alloy cermet coating, J. Mat. Res. Tech., 28, 2024, 97-109.
16. L.M. Wang, C.C. Chen, J.W. Yeh, S.T. Ke, The microstructure and strengthening mechanism of thermal spray coating $NixCo_{0.6}Fe_{0.2}CrySizAlTi_{0.2}$ high-entropy alloys, Mat. Chem. Phys., 126, 2011, 880-885.
17. W.C. Sun, P. Zhang, K. Zhao, M.M. Tian, Y. Wang, Effect of graphite concentration on the friction and wear of Ni-Al_2O_3/graphite composite coatings by a combination of electrophoresis and

electrodeposition, Wear., 342, 2015, 172-180.
18. C.X. Han, J.Q. Zhi, Z. Zeng, Y.S. Wang, B. Zhou, J. Gao, Y. Wu, Z.Y. He, X. Wang, S. Yu, Synthesis and characterization of nano-polycrystal diamonds on refractory high entropy alloys by chemical vapour deposition, Appl. Surf. Sci., 623, 2023, 157108.
19. N. Eißmann, B. Klöden, T. Weißgärber, B. Kieback, High-entropy alloy CoCrFeMnNi produced by powder metallurgy, Powd. Metal., 60, 2017, 184-197.
20. K.S.K.J. Reddy, L.P. Chokkakula, S.R. Dey, Strategies to engineer FeCoNiCuZn high entropy alloy composition through aqueous electrochemical deposition, Electrochim. Act., 453, 2023, 142350.
21. V. Soare, M. Burada, I. Constantin, D. Mitrică, V. Bădiliţă, A. Caragea, M. Târcolea, Electrochemical deposition and microstructural characterization of AlCrFeMnNi and AlCrCuFeMnNi high entropy alloy thin films, Appl. Surf. Sci., 358, 2015, 533-539.
22. F. Yoosefan, A. Ashrafi, S.M. Monir Vaghefi, Characterization of Co-Cr-Fe-Mn-Ni high-entropy alloy thin films synthesized by pulse electrodeposition: part 2: effect of pulse electrodeposition parameters on the wettability and corrosion resistance, Met. Mater. Int., 27, 2021, 106-117.
23. A. Aliyu, M.Y. Rekha, C. Srivastava, Microstructure-electrochemical property correlation in electrodeposited CuFeNiCoCr high-entropy alloy-graphene oxide composite coatings, Philos. Mag., 99, 2019, 718-735.
24. M. Tarakci, Plasma electrolytic oxidation coating of synthetic Al–Mg binary alloys, Mat. Charact., 62, 2011, 1214-1221.
25. J. Wu, W. Zhu, W. Yu, H. Ma, Y. Shao, Effect of TiC additions on the microstructure, mechanical and tribological properties of NbC-CoCrFeNiMn high entropy alloys cermets, Int. J. Ref. Met. Hard Mat., 112, 2023, 106141.
26. G.D. Chen, X.B. Liu, C.M. Yang, F.Z. Zhang, X.G. Li, J. Zheng, J. Liu, Strengthening mechanisms of laser cladding TiC/FeCoCrNiCu high-entropy composite coatings: Microstructure evolution and wear behaviors, Tribol. Int., 199, 2024, 109979.
27. Z. Ghaferi, K. Raeissi, M.A. Golozar, H. Edris, Characterization of nanocrystalline Co–W coatings on Cu substrate, electrodeposited from a citrate-ammonia bath, Surf. Coat. Technol., 206 2011, 497-505.
28. M. Mohan, U. Pandel, K. Kumar, Phase composition, surface chemistry and electrochemical studies of electrodeposited AlMnFeCuNi high entropy alloy composite coatings incorporated with carbon nanotubes, Mat. Res. Exp., 11, 2024, 046403.
29. L. Benea, N. Caron, O. Raquet, Tribological behavior of a Ni matrix hybrid nanocomposite reinforced by titanium carbide nanoparticles during electro-codeposition, RSC Adv., 6, 2016, 59775-59783.
30. T. Zhu, H. Wu, R. Zhou, N. Zhang, Y. Yin, L. Liang, W. Huang, Microstructures and tribological properties of TiC reinforced FeCoNiCuAl high-entropy alloy at normal and elevated temperature, Met., 10, 2020, 387.
31. C. Zhao, H. Zhu, Z. Xie, In-situ TiC particles strengthen and ductilize $Fe_{1.2}MnNi_{0.8}Cr$ high entropy alloy, Intermet., 140, 2022, 107398.
32. W.R. Osório, C.M. Freire, A. Garcia, The effect of the dendritic microstructure on the corrosion resistance of Zn-Al alloys, J. Alloy. Comp., 397, 2005, 179-191.
33. X. Qiu, Microstructure and mechanical properties of CoCrFeNiMo high-entropy alloy coatings, J. Mat. Res. Tech., 9, 2020, 5127-5133.